The Astrophysical Journal, 572:1077–1082, 2002 June 20

DISCOVERY OF SOFT X-RAY EMISSION FROM IO, EUROPA, AND THE IO PLASMA TORUS

Ronald F. Elsner,[1] G. Randall Gladstone,[2] J. Hunter Waite,[3] Frank J. Crary,[3] Robert R. Howell,[4] Robert E. Johnson,[5] Peter G. Ford,[6] Albert E. Metzger,[7] Kevin C. Hurley,[8] Eric D. Feigelson,[9] Gordon P. Garmire,[9] Anil Bhardwaj,[10] Denis C. Grodent,[3] Tariq Majeed,[2] Allyn F. Tennant,[1] and Martin C. Weisskopf[1]

Received 2001 November 19; accepted 2002 February 27

ABSTRACT

We report the discovery of soft (0.25–2 keV) X-ray emission from the Galilean satellites Io and Europa, probably Ganymede, and from the Io Plasma Torus (IPT). Bombardment by energetic (greater than 10 keV) H, O, and S ions from the region of the IPT seems to be the likely source of the X-ray emission from the Galilean satellites. According to our estimates, fluorescent X-ray emission excited by solar X-rays, even during flares from the active Sun, charge-exchange processes, previously invoked to explain Jupiter's X-ray aurora and cometary X-ray emission, and ion stripping by dust grains fail to account for the observed emission. On the other hand, bremsstrahlung emission of soft X-rays from nonthermal electrons in the few hundred to few thousand eV range may account for a substantial fraction of the observed X-ray flux from the IPT.

Subject headings: planets and satellites: individual (Io, Europa, Jupiter) — X-rays: general

1. INTRODUCTION

Imaging and spectral data from the infrared through the extreme ultraviolet provide important information on the makeup of the surfaces and atmospheres of the Galilean satellites Io, Europa, Ganymede, and Callisto (Carlson et al. 1999; Barth et al. 1997; Hall et al. 1998), discovered by Galileo Galilei in 1610, and of the Io Plasma Torus (IPT; Hall et al. 1994; Woodward, Scherb, & Roesler 1997; Gladstone & Hall 1998). Here we report the results of high spatial resolution X-ray observations of the Jovian system with the *Chandra X-Ray Observatory*, showing that the Galilean satellites and the IPT are also X-ray emitters, and we discuss the physical processes that may contribute.

2. OBSERVATIONS

The *Chandra X-Ray Observatory* (Weisskopf et al. 2000) observed the Jovian system on 1999 November 25–26 with the Advanced CCD Imaging Spectrometer (ACIS), in support of the *Galileo* flyby of Io, and on 2000 December 18 with the imaging array of the High Resolution Camera (HRC-I), in support of the *Cassini* flyby of Jupiter (Gladstone et al. 2002). During the ACIS observations, spanning 86.4 ks, the telescope focus and the planet were placed on the back-side–illuminated CCD designated S3 in order to take advantage of this CCD's sensitivity to low-energy X-rays. The spacecraft was repointed four times to allow for the planet's motion and was always oriented to allow the planet to move along the CCD's second node. These data were corrected for charge transfer inefficiency effects (Townsley et al. 2000), and only the standard *ASCA* grades 0, 2, 3, 4, and 6 were retained, in order to reduce the background induced by charged particles. Charge transfer inefficiency refers to the loss of charge during CCD readout for pixels farthest away from the readout node, leading to a low estimate for the event energy. Event grades depend on the distribution of charge induced by the event about the center pixel. X-ray and charge particle events produce different event grade distributions, allowing a powerful way to reduce unwanted background events. One ACIS pixel is $0\farcs492 \times 0\farcs492$, and the half-power diameter of the *Chandra* system level point-spread function is about $0\farcs8$. No repointings were necessary during the HRC-I observations, spanning 36.0 ks (approximately one rotation of Jupiter), because of the instrument's larger field of view and the observation's shorter length. One HRC-I pixel is $0\farcs1318 \times 0\farcs1318$.

Although the ACIS S3 optical filter is optically thick to optical light, there is an interference peak in its transmission near ~9000 Å (~1.4 eV) that is likely to affect ACIS S3 observations of solar system objects and nearby bright late-type stars. Indeed, the ACIS S3 data for Jupiter were compromised by the throughput in low-energy channels of large numbers of optical photons from the planet's bright disk. To eliminate this problem for our analysis, all events within $34\farcs4$ (~1.4 times Jupiter's radius) of the planet's center were removed from the data. In any event, removal of this data is required for analysis of the Galilean satellites in order to avoid contamination by events associated with Jupiter. The planet's optical emission also produced a bump in the ACIS bias frame, and all events within $34\farcs4$ of the center of this bump were removed from the data. For sufficiently bright

[1] Space Science Department, NASA Marshall Space Flight Center, SD50, Huntsville, AL 35812.
[2] Department of Space Science, Southwest Research Institute, P.O. Drawer 28510, San Antonio, TX 78228.
[3] Department of Atmospheric, Oceanic and Space Sciences, University of Michigan, Ann Arbor, MI 48109.
[4] Department of Physics and Astronomy, University of Wyoming, P.O. Box 3905, University Station, Laramie, WY 82071.
[5] Department of Engineering Physics, Thornton Hall, University of Virginia, Charlottesville, VA 22903.
[6] Center for Space Research, Massachusetts Institute of Technology, Cambridge, MA 02139.
[7] Jet Propulsion Laboratory, Pasadena, CA 91109.
[8] Space Science Laboratory, University of California, Berkeley, CA 94720.
[9] Department of Astronomy and Astrophysics, 525 Davey Laboratory, Pennsylvania State University, State College, PA 16802.
[10] Space Physics Laboratory, Vikram Sarabhai Space Centre, Trivandrum, India.

X-ray sources, X-ray events occurring during the 41 ms necessary to read out each 3.2 s ACIS accumulation appear as a streak, or trailed image, in the data. For our ACIS Jupiter observations, optical photons from the planet's disk do not contribute to a trailed image, as 41 ms is too short a time for sufficient accumulation to mimic an X-ray event. The trailed image from Jupiter's true X-ray events is a small effect for $E >\sim 440$ eV, where we have reasonably accurate knowledge of Jupiter's X-ray spectrum. From an extrapolation of Jupiter's X-ray spectrum to lower energies, we infer that the trailed image is also not a dominant effect for our analysis of the IPT at energies down to 250 eV. The trailed image is unimportant for our analysis of X-ray emission from the Galilean satellites. Since we wished to remove X-ray events associated with Jupiter, we removed events within 34″.4 of the planet's center from the HRC-I data.

2.1. *The Galilean Satellites*

In order to search for emission from each Galilean satellite, we removed *Chandra*'s orbital motion and transformed the data into a comoving frame using an ephemeris obtained from the Jet Propulsion Laboratory. The size of the detect cells was set equal to the root sum square of the satellite's radius and 2″. For the background, we determined an average number of events per detect cell in a larger region around the satellite in its own frame. This region was 98″.9 × 98″.9 for ACIS and 98″.7 × 98″.7 for HRC-I. The number of events within the detect cell centered on each satellite compared with this background value determines a probability of chance occurrence according to Poisson statistics. The results of this analysis appear in Table 1. Since these objects move across the field of view, *Chandra*'s spatial resolution at their position varies, so in each case we also compared the radial distribution of events around the satellite with that around 100 points chosen at random in the surrounding region. Io is detected in both the ACIS and HRC-I data, while Europa is detected in the ACIS data only. Ganymede appears at the 99% confidence level in the ACIS data. A simple calculation of joint probabilities confirms the detection of Io and Europa, with results that we find tantalizing for Ganymede and Callisto. The nominal energies of the X-ray events range from 300 to 1890 eV and seem to show a clustering between 500 and 700 eV. The mean energy, weighted appropriately by *Chandra*'s effective area, of the events is 515 and 664 eV for Io and Europa, respectively. The corresponding estimated energy flux at the telescope and emitted power from the satellite are 4.1×10^{-16} ergs s^{-1} cm^2 and 2.0 MW for Io, and 3.0×10^{-16}

TABLE 1
X-Ray Emission from the Galilean Satellites

Parameter	Io	Europa	Ganymede	Callisto
ACIS[a] (1999 Nov 25–26)				
N_{moon}[b]	11	12	5	3
$\langle N_{bkgd}\rangle$[c]	1.26	1.94	1.25	1.27
Pr[$N \geq N_{moon}$][d]	1.03×10^{-8}	1.46×10^{-7}	9.09×10^{-3}	0.137
HRC-I (2000 Dec 18)				
N_{moon}[b]	10	3	3	6
$\langle N_{bkgd}\rangle$[e]	2.88	3.08	3.58	3.24
Pr[$N \geq N_{moon}$][d]	8.06×10^{-4}	0.595	0.694	0.110
Joint (ACIS + HRC-I)				
Pr[$N \geq N_{moon}$][d]	3.47×10^{-9}	2.36×10^{-4}	0.116	0.041

[a] 250–2000 eV.
[b] Number of counts in detect cell centered on the satellite.
[c] Average number of counts per detect cell in a 98″.9 × 98″.9 region surrounding the satellite.
[d] Probability of chance occurence for $N \geq N_{moon}$.
[e] Average number of counts per detect cell in a 98″.7 × 98″.7 region surrounding the satellite.

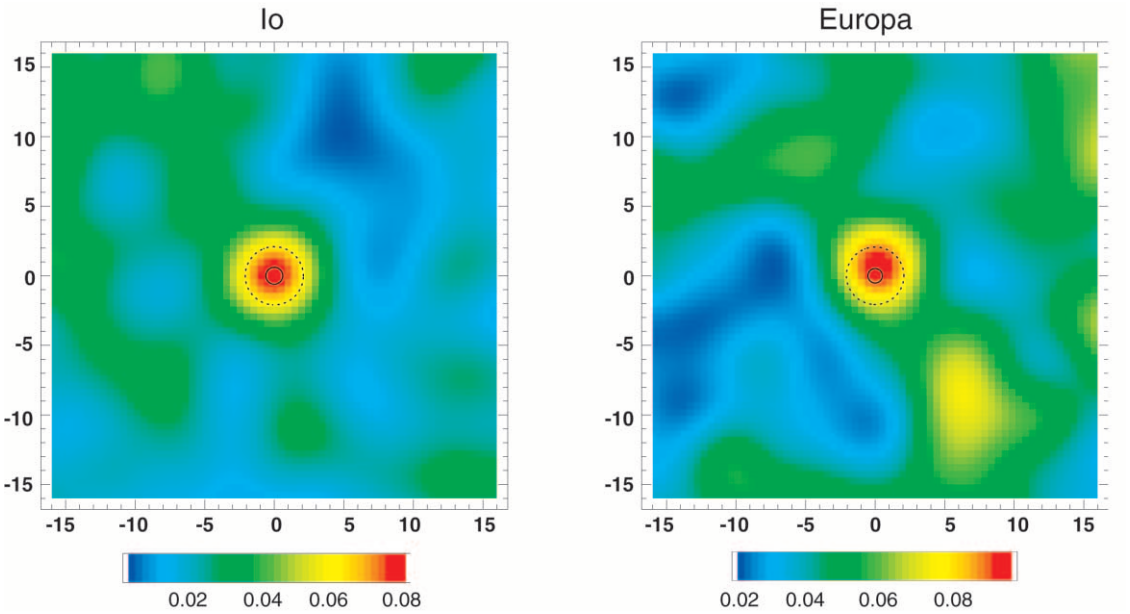

Fig. 1.—ACIS images of Io and Europa (250 eV < E < 2000 eV). The images have been smoothed by a two-dimensional Gaussian with $\sigma = 2''.46$ (5 ACIS pixels). The axes are labeled in arcsec (1″ ≃ 2995 km), and the scale bar is in units of smoothed counts per image pixel (0″.492 × 0″.492). The solid circle shows the size of the satellite (the radii of Io and Europa are 1821 and 1560 km, respectively) and the dotted circle the size of the detect cell.

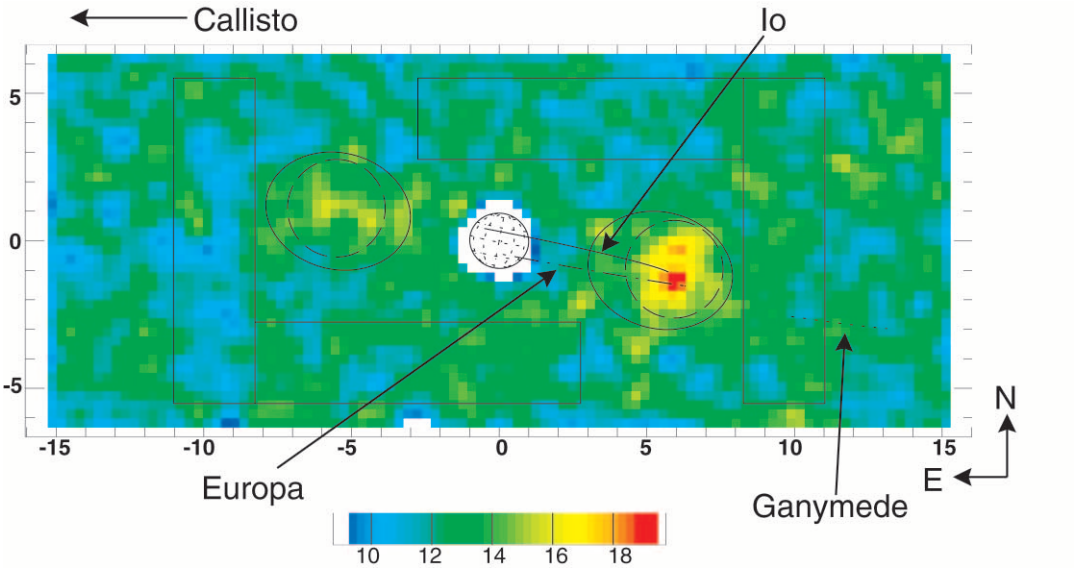

FIG. 2.—HRC-I image of the IPT (2000 December 18). The image has been smoothed by a two-dimensional Gaussian with $\sigma = 7\farcs38$ (56 HRC-I pixels). The axes are labeled in units of Jupiter's radius, R_J, and the scale bar is in units of smoothed counts per image pixel ($7\farcs38 \times 7\farcs38$). The paths traced by Io (*solid line*, semimajor axis 5.9 R_J), Europa (*dashed line*, semimajor axis 9.5 R_J), and Ganymede (*dotted line*, semimajor axis 15.1 R_J) are marked on the image. Callisto (semimajor axis 26.6 R_J) is off the image to the dawn side, although the satellite did fall within the full microchannel plate field of view. For this observation, Jupiter's equatorial radius corresponds to $23\farcs9$. The regions bounded by rectangles were used to determine background. The regions bounded by dashed circles or solid ellipses were defined as source regions.

ergs s^{-1} cm^2 and 1.5 MW for Europa. Figure 1 shows smoothed ACIS images of Io and Europa.

2.2. *The Io Plasma Torus*

Figure 2 shows the HRC-I image zoomed back from Jupiter, in the planet's frame of reference. There is a region of diffuse emission on the dusk side of the planet, and a fainter region of diffuse emission on the dawn side of the planet. This morphology is similar to the dawn-dusk asymmetry seen in *Extreme Ultraviolet Explorer* (*EUVE*) data (Hall et al. 1994; Gladstone & Hall 1998). The paths traced by Io, Europa, and Ganymede during the HRC-I observation are also shown. Io and Europa pass through the dusk-side region of diffuse X-ray emission. We associate these regions of diffuse emission with the IPT. The background-subtracted HRC-I count rates are 3.2×10^{-3} counts s^{-1} arcmin^2 on the dawn side of Jupiter and $5.6\text{–}7.1 \times 10^{-3}$ counts s^{-1} arcmin^2 on the dusk side of Jupiter. The larger rate for the dusk-side region applies to a circular source region of 1.36 arcmin^2 and the smaller to the larger elliptical source region of 2.43 arcmin^2 suggested by the ACIS observations. The rate for the dawn-side region applies to both the smaller and larger source regions.

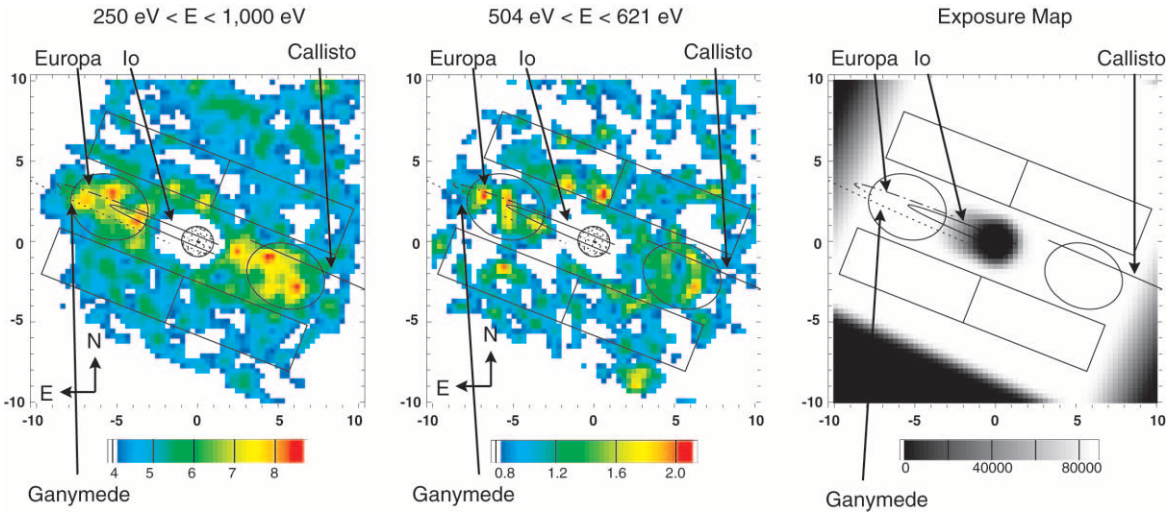

FIG. 3.—ACIS image of the IPT (1999 November 25–26) for 250 eV $< E <$ 1000 eV (*left*) and for 504 $< E <$ 621 eV (*center*). The image has been smoothed by a two-dimensional Gaussian with $\sigma = 7\farcs38$ (15 ACIS pixels). The axes are labeled in units of Jupiter's radius, R_J, and the scale bar is in units of smoothed counts per image pixel ($7\farcs38 \times 7\farcs38$). For this observation, Jupiter's equatorial radius corresponds to $23\farcs8$. The paths traced by Io (*solid line on the dawn side*), Europa (*dashed line*), Ganymede (*dotted line*), and Callisto (*solid line on the dusk side*) are marked on the image. The regions bounded by rectangles were used to determine background. The regions bounded by ellipses were defined as source regions. The exposure (*right*) varies over the image because four overlapping observations were concatenated, and because we discarded data within $34\farcs4$ of Jupiter's center or within $34\farcs4$ of the center of the bump in the bias frame.

Figure 3 shows the ACIS image zoomed back from Jupiter, in the planet's frame of reference over the energy ranges 250–1000 eV (*left panel*) and 504–621 eV (*center panel*). Because this image was produced from four overlapping observations, and also because of the instrumental effects discussed above, we show an exposure map (*right panel*) for the image in Figure 3. The area of low exposure around Jupiter is due to the removal of events within 34″.4 of the planet's center or within 34″.4 of the center of the bump in the bias frame. The ACIS image also shows regions of diffuse emission on the dawn side and dusk side of the planet. The paths traced by Io, Europa, Ganymede, and Callisto during the ACIS observations are also shown. In this case, Io and Europa pass through the dawn-side region of diffuse X-ray emission. The ACIS 250–1000 eV background-subtracted count rates are 1.7×10^{-3} counts s^{-1} arcmin^2 on both the dawn side and dusk side of Jupiter. However, the 504–621 eV image shows significant asymmetry, with stronger emission on the dawn side, where Io and Europa were located during the ACIS observations. The HRC-I image also shows stronger emission on the side (dusk in that observation) where Io and Europa were located during that observation. The narrowband ACIS image also shows emission to the north of Jupiter, which we do not associate with the IPT.

Both a simple power law and thermal bremsstrahlung give statistically acceptable fits to the background-subtracted 250–1000 eV ACIS IPT spectrum (see Table 2 and Fig. 4). However, adding a single Gaussian line does significantly improve these fits. The central energy of the Gaussian is very close to a strong O VII line at 574 eV. Lines from other oxygen charge states may also contribute. The background-subtraction procedure correctly removed instrumental lines such as Si Kα at 1.74 keV. The 250–1000 eV energy flux at the telescope from the IPT (within the ovals marked on Fig. 3) is 2.4×10^{-14} ergs s^{-1} cm^2, corresponding to a luminosity of 0.12 GW, and is approximately evenly divided between the dawn side and dusk side. The apparent X-ray line emission around 570 eV originates predominantly on the dawn side of the planet. *EUVE* observations in 1993 (Hall et al. 1994; Gladstone & Hall 1998) determined an IPT energy flux of $(7.2 \pm 0.2) \times 10^{-11}$ ergs s^{-1} cm^2 over the interval 370–735 Å (17–34 eV). This flux is ~3000 times that inferred from the *Chandra* data over the interval 250–1000 eV.

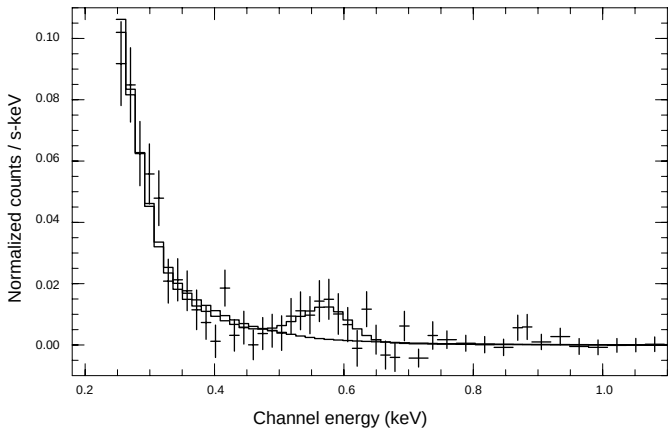

FIG. 4.—Background-subtracted ACIS IPT spectrum, normalized counts s^{-1} keV vs. channel energy in keV, for 0.25 keV $< E <$ 1.0 keV, together with the power-law and power-law plus Gaussian model fits given in Table 2.

TABLE 2
SPECTRAL FITS TO ACIS IPT DATA (250 eV $< E <$ 1000 eV)

Parameter	Value
Power Law[a]	
γ	6.3 (+0.4/−0.4)
K (10^{-10} counts s^{-1} eV cm^2)	1.5 (+1.8/−0.9)
Power Law Plus Gaussian Line[b]	
γ	6.8 (+0.5/−0.4)
K (10^{-10} counts s^{-1} eV cm^2)	0.8 (+0.6/−0.4)
E_{line} (eV)	569 (+11/−13)
σ (eV)	0 (+25)
A (10^{-6} counts s^{-1} cm^2)	3 (+1/−1)
Thermal Bremsstrahlung[c]	
T (eV)	60 (+7/−5)
$EM^d/10^{40}$	4.9 (+2.4/−1.9)
Thermal Bremsstrahlung Plus Gaussian Line[e]	
T (eV)	56 (+6/−5)
$EM^d/10^{40}$	7 (+4/−2)
E_{line} (eV)	567 (+10/−12)
σ (eV)	0 (+28)
A (10^{-6} counts s^{-1} cm^2)	4 (+1/−1)

[a] $dN/dE = KE^{-\gamma}$, $\chi^2 = 48$ for 51 degrees of freedom.
[b] $dN/dE = KE^{-\gamma} + (A/\sigma\sqrt{2\pi}) \exp[-(E - E_{line})^2/2\sigma^2]$, $\chi^2 = 34$ for 48 degrees of freedom.
[c] $dN/dE = EMf_{brems}(E, T)$, $\chi^2 = 50$ for 51 degrees of freedom.
[d] $\int n_e n_i dV$, with n_e and n_i the electron and ion densities in units of cm^{-3}.
[e] $dN/dE = EMf_{brems}(E, T) + (A/\sigma\sqrt{2\pi}) \exp[-(E - E_{line})^2/2\sigma^2]$, $\chi^2 = 31$ for 48 degrees of freedom.

3. DISCUSSION

We have observed X-rays that originate from the IPT, the Galilean satellites Io and Europa, and probably Ganymede. Two known energy sources are available to drive these processes: (1) the solar X-ray flux and (2) the energetic particle populations in the region of the IPT. Furthermore, we must consider the X-ray production processes that originate from the surfaces of the Galilean satellites as distinct and different from the X-ray processes that lead to emission from the IPT.

3.1. *The Galilean Satellites*

We first consider the surface emissions from Io and Europa. Based on the results of model calculations (Peres et al. 2000), the energetic particles that constitute the outer radiation belts of Jupiter and that are found within the IPT provide energy fluxes to the surfaces of Io and Europa that are ~20 and ~110, respectively, times larger than the solar X-ray flux during solar maximum conditions with active flares. We show below that the relevant incident particles and energies are those that deposit most of their energy in the top ~10 μm of the surface. Irradiation models show that ion energy losses dominate that from electrons in this layer (Paranicas, Carlson, & Johnson 2001; Cooper et al. 2001). Even along Europa's trailing hemisphere, we suspect that the total energetic ion dose dominates the energetic electron

dose down to about tens of microns in depth, below which point the situation is reversed (Paranicas et al. 2002). This, together with the clustering of X-ray event energies between 500 and 700 eV, suggests that the observed emission cannot be due to electron bremsstrahlung. Since the cross sections for interaction and the efficiency for X-ray production from energetic ion impact and from fluorescence excited by solar X-rays are comparable, we conclude that the X-ray emission from Io and Europa is ultimately powered by the energetic ion population in the IPT. The surfaces of the Galilean satellites are exposed to bombardment by energetic ions diffusing radially inward through the region of the IPT. The incident flux is made up of energetic H, O, and S ions (Paranicas et al. 2002; Cooper et al. 2001). Although Io and Europa have ionospheres that deflect low-energy ions, more energetic ions with large gyroradii will reach their surfaces and produce X-rays through particle-induced X-ray emission (Johansson, Campbell, & Malmqvist 1995). In fact, the large gyroradii for the X-ray–producing ions means that the effective cross section of the Galilean satellites to IPT ions is larger than their physical size (Pospieszalska & Johnson 1989).

Io's atmosphere arises from sublimation of surface SO_2 frost, sputtering on the surface by Jovian magnetospheric particles and volcanic activity, with the latter perhaps being the dominant contributor. This atmosphere is patchy rather than uniform but can be expected to provide a lower limit to the energy of ions impacting the surface. Approximately 5 keV H^+, 40 keV O^+, and 60 keV S^+ ions penetrate an atmosphere with a column density of 10^{17} SO_2 molecules cm^{-2} (Lanzerotti et al. 1982); these limits fall between 1 and 10 keV for a column density of 10^{16} SO_2 molecules cm^{-2}. For comparison, electrons with energy greater than about 10 keV penetrate a column density of 10^{17} SO_2 molecules cm^{-2} (Michael & Bhardwaj 2000). The integrated ion energy flux at Europa for H, O, and S above 10 keV (Paranicas et al. 2002; Cooper et al. 2001) is $\sim 10^{10}$ keV s^{-1} cm^2. The energetic ion flux at Io is $\sim$5 times smaller, but is less well known than for Europa. The depth of the region of interest is limited by the absorption of escaping X-rays in the surface. For Europa's water ice surface, absorption in oxygen dominates, while for Io's surface, absorption in oxygen is complemented by that in silicon, sulfur, and other elements. Oxygen Kα X-rays at 525 eV in ice have an optical depth of unity at about 9.5 μm, implying an oxygen column density of 3.2×10^{19} cm^{-2}. For incident protons with energy greater than $\sim$300 keV and an oxygen target, the cross section for X-ray production is flat with energy and is $\sim 10^{-21}$ cm^2, implying an X-ray yield per proton of $\sim$0.01 for Europa. Similarly, the presence of sulfur dioxide (atomic weight 64) rather than water (atomic weight 18) suggests an X-ray yield per proton of $\sim$0.04 for Io. These yield estimates are uncertain; accurate estimates require more detailed work. The production cross sections for energetic O and S ions are larger, but the corresponding penetration depths are smaller, suggesting similar yields. Dividing the ion energy flux by an assumed average ion energy of 100 keV and multiplying by the X-ray yield per ion gives an X-ray surface emission rate of 1.5×10^6 photons s^{-1} cm^2 for Europa and 1.2×10^6 photons s^{-1} cm^2 for Io. If 10% of these photons are O K-shell X-rays with energies around 525 eV, then the predicted power in O K-shell X-rays is 3.9×10^{13} and 4.2×10^{13} ergs s^{-1} for Europa and Io, respectively. The corresponding fluxes at the telescope are 8.1×10^{-16} and 8.7×10^{-16} ergs s^{-1} for Europa and Io, respectively. The fluxes predicted by these simple estimates are within a factor of $\sim$3 of the observed fluxes for Europa and Io. Despite these low flux levels, further observations with the *Chandra* and *XMM-Newton* X-ray observatories may eventually permit the identification of lines from individual heavy elements.

3.2. *The Io Plasma Torus*

Turning now to the IPT, we estimate its X-ray flux (in O K-shell lines from O, O^+, and O^{++}) from fluorescence caused by the X-ray flux from the Sun. We use the results of model calculations for X-ray emission from the flaring active Sun (Peres et al. 2000), normalized to the model X-ray luminosity in the energy band 0.1–10 keV, to determine the solar spectrum at Jupiter's orbit (the planet was 4.14 AU from the Earth and 4.96 AU from the Sun during the 1999 November 25–26 ACIS observations, and 4.12 AU from the Earth and 5.04 AU from the Sun during the 2000 December 18 HRC-I observations). Photoionization cross sections are from analytic fits to the results of calculations using the Hartree-Dirac-Slater method (Verner et al. 1993). For photoionization of oxygen ions at energies just above the K-edge, the cross sections are of the order of a few $\times$ 10^{-19} cm^2, decreasing with increasing energy roughly as $1/E^3$. For the fluorescent yield, we use the value for neutral oxygen (0.0083; Krause 1979). Galileo measured electron (Bagenal et al. 1997) and ion (Crary et al. 1998; Frank & Paterson 2000) densities above 1000 cm^{-3} in some regions of the IPT. Assuming the volume of a torus with semimajor axis equal to that of Io's orbit and diameter equal to Jupiter's equatorial diameter, and number densities in neutral oxygen and in ionized oxygen (mostly O^+) of 1000 cm^{-3}, we find a photon flux at the Earth of 2.6×10^{-7} photons s^{-1} cm^2 for the flaring active Sun. Our spectral fits require photon fluxes in the apparent line near 570 eV of $\sim 3 \times 10^{-6}$ photons s^{-1} cm^2, about an order of magnitude larger. We conclude that the observed X-ray emission from the IPT is not due to fluorescence excited by solar X-rays.

Charge-exchange processes have been invoked to explain Jupiter's X-ray aurora (Cravens et al. 1995; Bhardwaj & Gladstone 2000) and X-ray emission from comets (Cravens 1997; Dennerl 1999). As energetic ions diffuse inward through the region of the IPT, they are constantly subject to both electron stripping and charge exchange. Electron stripping generally has a higher probability than charge exchange above some crossover energy. The crossover energy is different for the different charge states, with higher charge states having a generally higher crossover energy. The crossover energy for an O VII ion, above which electron stripping is favored, occurs above 11 MeV (Cravens 1997). Ions below a few tens of keV rapidly charge exchange in the outer torus, become neutralized, and are lost from the Jupiter system (Mauk et al. 1998). These energetic neutrals have been recently observed by the *Cassini* spacecraft during its flyby of Jupiter (Krimigis et al. 2002). However, as the higher energy ions slowly diffuse radially inward through the plasma torus region, increasing numbers are driven to higher and higher charge states. In fact, we argue that all oxygen ions with energies over 16 MeV are fully stripped by the time they diffuse radially inward to 6 Jupiter radii near Io's orbit (where they are observed). Upon colliding with a torus neutral and undergoing charge exchange to O VII, such

ions can produce an X-ray photon at energies near 570 eV. From the Galileo Heavy Ion Counter experiment (Cohen et al. 2000), we find an integrated flux of oxygen ions above 16 MeV of 1.5×10^4 ions s^{-1} cm^2 . Combining this with an estimated charge-exchange cross section (Cravens et al. 1995) of 10^{-18} cm^2, an estimated neutral density of 30 cm^{-3}, and an estimated X-ray emission probability of 0.065, we obtain an X-ray volume production rate of 4.5×10^{-13} photons s^{-1} cm^3. Taking the same IPT volume as assumed for our fluorescence estimate, we find a photon flux at Earth of $\sim 4 \times 10^{-10}$ photons s^{-1} cm^2, approximately 4 orders of magnitude smaller than the required flux near 570 eV. Similar considerations show that ion stripping by dust grains leading to X-ray emission also fails to explain the apparent line emission.

A large fraction of the IPT X-ray flux may result from bremsstrahlung radiation from nonthermal electrons. Above a few tens of eV, the electrons' energy distribution is well described by a power law rather than a Maxwellian (Sittler & Strobel 1987; Meyer-Vernet, Moncuquet, & Hoang 1995). These nonthermal electrons play a critical role in setting the charge state of the Io torus and the energy balance of the IPT. Estimates of cooling from electron-impact excited UV emissions and heating from Coulomb collisions with ions (Smith et al. 1988) show the need for a large, additional source of energy. The nature of this energy source remains speculative, but it may result from wave-particle heating (Barbosa 1994) or inward diffusion of energetic ions and electrons from Jupiter's middle and outer magnetosphere (Smith et al. 1988). Previous remote sensing observations have provided limited data on these nonthermal electrons, since UV and longer wavelength emissions are primarily sensitive to electrons with energies below a few eV.

Bremsstrahlung emission of soft X-rays is, on the other hand, produced by the nonthermal electrons in the few hundred to few thousand eV range. Based on the in situ *Ulysses* observations, we assume the electrons are in a κ, or generalized Lorentzian, distribution, with a temperature of 10 eV and an index of $\kappa = 2.4$ (Meyer-Vernet et al. 1995). Using this distribution and the Bethe-Heitler cross section for bremsstrahlung emission (with Sommerfeld-Elwert correction), we numerically calculate the source rate and spectrum. At a density of 2000 cm^{-3}, typical of the IPT, the source rate is 6×10^{-18} ergs cm^{-3} s. Integrated over the entire IPT, the radiated X-ray power between 250 and 1000 eV is approximately 3×10^7 W, or roughly one-third of the observed signal. The predicted shape of the bremsstrahlung spectrum is harder than the measured $1/E^{6.8}$ spectrum, indicating that some of the flux near 250 eV is probably an extension of the far-ultraviolet (FUV) emission from the IPT (Hall et al. 1994; Gladstone & Hall 1998).

4. CONCLUSIONS

Chandra X-Ray Observatory observations have shown that Io and Europa, and probably Ganymede, emit soft X-rays with 0.25–2.0 keV luminosities ~1–2 MW. This emission is likely to result from bombardment of their surfaces by energetic (greater than 10 keV) H, O, and S ions from the region of the IPT. The IPT itself emits soft X-rays with a 0.25–1.0 keV luminosity ~0.1 GW. Most of this emission appears at the low end of the energy band, but an unresolved line or line complex is apparent in the spectrum at an energy consistent with oxygen. The origin of the IPT X-ray emission is uncertain, but bremsstrahlung from nonthermal electrons may account for a significant fraction of the continuum X-rays.

Further X-ray observations and more detailed modeling are needed to probe more deeply into the origin and properties of the X-ray emission from the Galilean satellites and from the Io Plasma Torus and their implications for the Jovian magnetosphere.

The authors thank L. Townsley for making CTI corrections to the ACIS data and F. Bagenal for helpful communications.

REFERENCES

Bagenal, F., et al. 1997, Geophys. Res. Lett., 24, 2119
Barbosa, D. D. 1994, J. Geophys. Res., 99, 11079
Barth, L. A., et al. 1997, Geophys. Res. Lett., 24, 2147
Bhardwaj, A., & Gladstone, G. R. 2000, Rev. Geophys., 38, 295
Carlson, R. W., et al. 1999, Science, 283, 2062
Cohen, C. M. S., et al. 2000, J. Geophys. Res., 105, 7775
Cooper, J. F., Johnson, R. E., Mauk, B. H., Garrett, H. B., & Gehrels, N. 2001, Icarus, 149, 133
Crary, F. J., Bagenal, F., Frank, L. A., & Paterson, W. R. 1998, J. Geophys. Res., 103, 29359
Cravens, T. E. 1997, Geophys. Res. Lett., 24, 105
Cravens, T. E., Howell, E., Waite, J. H., & Gladstone, G. R. 1995, J. Geophys. Res., 100, 17153
Dennerl, K. 1999, At. Phys., 16, 361
Frank, L. A., & Paterson, W. R. 2000, J. Geophys. Res., 105, 25363
Gladstone, G. R., & Hall, D. T. 1998, J. Geophys. Res., 103, 19927
Gladstone, G. R., et al. 2002, Nature, 415, 1000
Hall, D. T., Feldman, P. D., McGrath, M. A., & Strobel, D. F. 1998, ApJ, 499, 475
Hall, D. T., et al. 1994, ApJ, 426, L51
Johansson, S. A. E., Campbell, J. L., & Malmquist, K. G. 1995, Particle-Induced X-Ray Emission Spectrometry (PIXE) (New York: Wiley)
Krause, M. O. 1979, J. Phys. Chem. Ref. Data, 8, 307
Krimigis, S. M., et al. 2002, Nature, 415, 994
Lanzerotti, L. J., et al. 1982, ApJ, 259, 920
Mauk, B. H., et al. 1998, J. Geophys. Res., 103, 4715
Meyer-Vernet, N., Moncuquet, M., &. Hoang, S. 1995, Icarus, 116, 202
Michael, M., & Bhardwaj, A. 2000, Geophys. Res. Lett., 27, 3137
Paranicas, C., Carlson, R. W., & Johnson, R. E. 2001, Geophys. Res. Lett., 28, 673
Paranicas, C., Ratliff, J. M., Mauk, B. H., Cohen, C., & Johnson, R. E. 2002, Geophys. Res. Lett., 29, 14127
Peres, G., Orlando, S., Reale, F., Rosner, R., & Hudson, H. 2000, ApJ, 528, 537
Pospieszalska, M. K., & Johnson, R. E. 1989, Icarus, 78, 1
Sittler, E. C., & Strobel, D. F. 1987, J. Geophys. Res., 92, 5741
Smith, R. A., Bagenal, F., Chang, A. F., & Strobel, D. F. 1988, Geophys. Res. Lett., 15, 545
Townsley, L. K., Broos, P. S., Garmire, G. P., & Nousek, J. A. 2000, ApJ, 534, L139
Verner, D. A., Yakovlev, D. G., Band, I. M., & Trzhaskovskaya, M. B. 1993, At. Data Nucl. Data Tables, 55, 233
Weisskopf, M. C., Tananbaum, H. D., Van Speybroeck, L. P., & O'Dell, S. L. 2000, Proc. SPIE, 4012, 2
Woodward, R. C., Scherb, F., & Roesler, F. L. 1997, ApJ, 479, 984